Large Phosphorus Hyperfine Coupling as a Sensitive Tool for Studying Molecular Dynamics: ESR and Molecular Mechanics Studies of Ring Interconversion in the *cis*-2,5-Diphosphoryl-2,5-dimethyl-pyrrolidinoxyl Radical

Antal Rockenbauer,[†] Anouk Gaudel-Siri,[‡] Didier Siri,[‡] Yves Berchadsky,[§] François Le Moigne,[§] Gilles Olive,[§] and Paul Tordo*[,§]

Chemical Research Center, Institute of Chemistry H-1075 Budapest, Pusztaszeri 59, Hungary, Laboratoire de Chimie Théorique et Modélisation Moléculaire, UMR 6517, CNRS-Universités d'Aix-Marseille I et III, Case D42, 13397 Marseille, Cédex 20, France, and Laboratoire Structure et Réactivité des Espèces Paramagnétiques, UMR 6517, CNRS-Universités d'Aix-Marseille I et III, Case 521, 13397 Marseille, Cédex 20, France

Received: June 5, 2002; In Final Form: January 20, 2003

ESR spectra of *cis*- and *trans*-β-diphosphorylated pyrrolidine-*N*-oxyl radicals, **c-1** and **t-1**, were studied in liquid and frozen solution. The expected 1:2:1 triplet (a_P (2)) of the 1:1:1 triplet (a_N) was observed for **t-1**; however, for **c-1**, the inner lines of the 1:2:1 triplet showed a dramatic broadening characteristic of chemical exchange between two equivalent conformations. Owing to the large difference in the hyperfine splitting constants (hfsc) of the exchanging phosphorus ($\Delta a_P \approx 21$ G), the coalescence temperature was unusually high (193 K, in *n*-pentane), and the potential barrier for ring interconversion (10.5 kJ mol^{-1}) was easily obtained from the temperature dependence of the exchange rate. This value was in very good agreement with the value obtained for an empirical pseudorotational potential (11 kJ mol^{-1}) that was adjusted to fit the temperature dependence of the phosphorus hfsc. For **c-1**, molecular mechanics calculations gave similar characteristics for the pseudorotational potential and indicated the existence of two identical minima with distorted geometries lying between $^3T_4$ and ^3E or $^4T_3$ and E_3. For **t-1**, only the $^3T_4$ conformer was found to be significantly populated. Frozen solution spectra showed that the phosphorus hfsc anisotropy is higher when the C−P bond is pseudoaxial; this result can be explained by a geometry-dependent delocalization of the unpaired electron into the phosphorus 3p orbitals.

Introduction

Because of the biological importance of various five-membered rings such as those of ribose rings in nucleic acids[1] and proline residues in peptides and proteins,[2] there is still considerable interest in determining the conformational states of five-membered rings. Pyrrolidine-*N*-oxyl radicals (Scheme 1) form an important class of five-membered ring radicals. If their dismutation is prevented by the absence of hydrogens on the α carbons, then most of these radicals are chemically stable, and different approaches have been developed to investigate their conformational behavior.[3,4]

The conformers of five-membered rings can be close to either envelope (E) or twist (T) geometries (Figure 1). Conversion among the various conformers is usually thought to occur through pseudorotation. Spectroscopic techniques often fail to give reliable information on the heights and positions of barriers to interconversion, except for few simple molecules when the microwave technique is applicable.[5] As compared to six-membered rings containing six σ bonds (sp^3 carbon or nitrogen atoms) where energetically well-separated (ΔG^0 is ca. 20 kJ mol^{-1}) and slowly interconverting (the interconversion frequency is less than 5×10^8 s^{-1} below room temperature) conformers exist,[6] the analogous five-membered rings are rather flexible, and interconversion is fast. (ΔG^0 does not exceed 10 kJ mol^{-1}, and the interconversion frequency is larger than 7×10^9 s^{-1} above 200 K.[7,8a]) This difference is evident in ESR spectroscopy studies where line-width alternation due to chemical exchange is often observed in the spectra of radicals centered on a six-membered ring. However, for the five-membered ring analogues, such phenomena were detected only in a few cases using the low-temperature matrix technique.[8] For five-membered ring radicals, the lack of line-width alternation is caused by the complete averaging of coupling constants due to the fast pseudorotation.

SCHEME 1

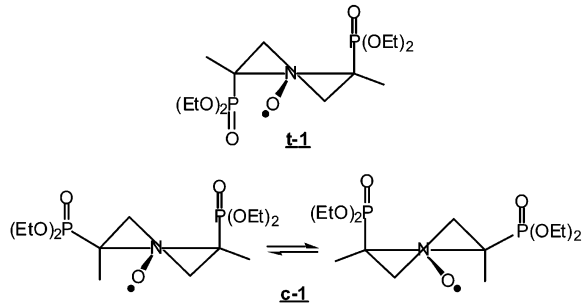

Line broadening resulting from chemical exchange depends on the square of the differences in the coupling constants for

* Corresponding author. E-mail: tordo@srepir1.univ-mrs.fr. Tel: 33 4 91 632 851.
[†] Institute of Chemistry.
[‡] Laboratoire de Chimie Théorique et Modélisation Moléculaire, CNRS-Universités d'Aix-Marseille I et III.
[§] Laboratoire Structure et Réactivité des Espèces Paramagnétiques, CNRS-Universités d'Aix-Marseille I et III.

10.1021/jp0213351 CCC: $25.00
Published on Web 04/11/2003

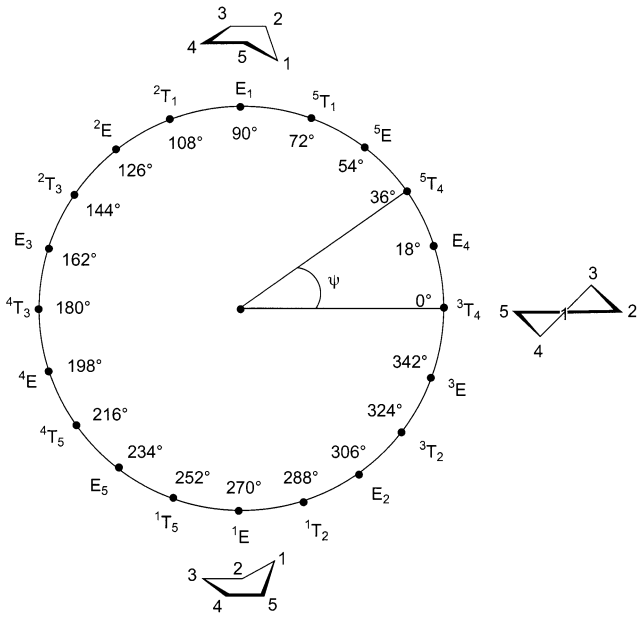

Figure 1. Usual representation of the pseudorotation of five-membered rings.

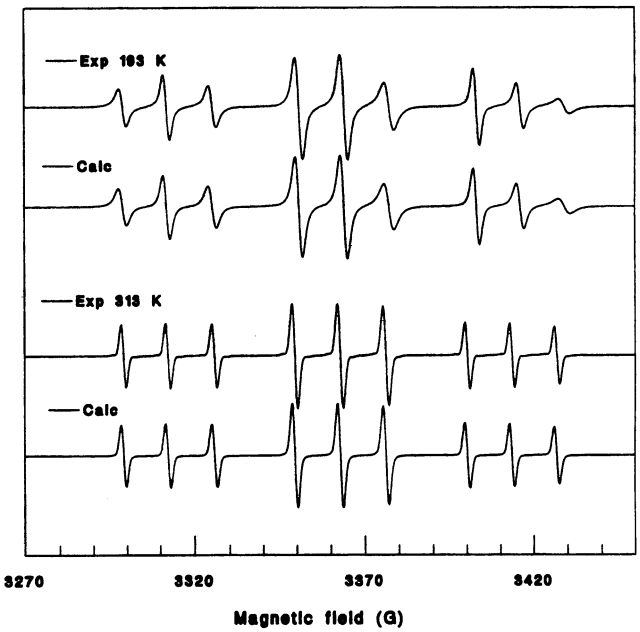

Figure 2. Experimental and calculated ESR spectra for **t-1**: 193 K (top) and 313 K (bottom).

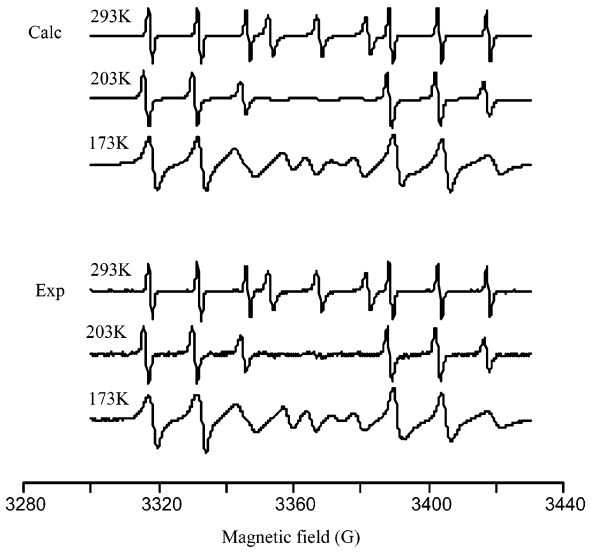

Figure 3. Experimental and calculated ESR spectra for **c-1** at different temperatures.

interconverting sites, and since β-phosphorus couplings are typically two or three times larger than the respective β-hydrogen couplings, the presence of a β-^{31}P atom in a free radical should enhance the chance to observe chemical exchange.

In our earlier studies, dramatic line-broadening effects were indeed observed on the ESR spectra of peroxyl radical adducts of 2-diethoxyphosphoryl-2-methyl-3,4-dihydro-2H-pyrrole-1-oxide (DEPMPO)[9a,b] as well as on those of geminal diphosphoryl-substituted pyrrolidinoxyl radicals.[9c] Interconversion between conformers with different ring geometries resulting from hindered rotation around the O−OR bond in the first case or the C−P bond in the second case[9c] can explain the observed line broadening. However, in both cases, the barrier for ring inversion does not represent the major contribution to the total barrier for interconversion, and thus the rate of ring inversion is not available from ESR experiments.

Because of the preference of the pyrrolidinoxyl radicals for $^3T_4$ and $^4T_3$ twist conformations[3] and the preference of the diethoxyphosphoryl group for axial geometry,[3c] no ring interconversion was observed for *trans*-2,5-diethoxy-phosphoryl-2,5-dimethyl-pyrrolidinoxyl nitroxide **t-1** (Scheme 1, Figure 2). However, for *cis*-2,5-diethoxyphosphoryl-2,5-dimethyl-pyrrolidinoxyl nitroxide **c-1** (Scheme 1), one phosphoryl substituent occupies the preferred axial geometry, and the second is forced to the less stable equatorial orientation. As a consequence, a double minimum is expected in the pseudorotational itinerary of the pyrrolidinoxyl ring.

In the present paper, we give a complete analysis of the ESR spectra of **c-1** recorded over a large temperature range. To obtain reliable calculated data, liquid and frozen solution spectra were simulated by an automatic parameter-fitting procedure.[10] The study of the influence of temperature on the interconversion rate yielded the thermodynamic parameters of the process. We also considered the influence of solvent molecules on the chemical exchange. Moreover, in frozen solution, where different ring geometries can be fixed by solvation, we examined the possibility of phase transition due to molecular rearrangements in the coordination sphere.

Finally, to have a complete description of the pseudorotational itinerary, conformational analysis of **t-1** and **c-1** was performed using molecular mechanics calculations. In this approach, the influence of rotation around the C−P bonds was considered.

Results and Discussion

ESR Spectra. The ESR spectrum of **t-1** consisted of a large 1:2:1 triplet due to coupling with two equivalent phosphorus nuclei, each line being further split into the 1:1:1 triplet of ^{14}N. As shown in Figure 2, no chemical exchange was observed in the temperature range between 193 and 313 K. [9c]

At elevated temperature, the ESR spectra of **t-1** and **c-1** are similar. However, for the cis isomer, the inner lines of the 1:2:1 triplet showed a dramatic broadening that is characteristic of a chemical exchange (Figure 3). A decrease in the temperature increased the broadening of the inner lines, whereas lines in the wings remained sharp. Inner and outer lines had nearly identical amplitudes at 253 K, and coalescence was achieved at 193 K. Below this temperature, new lines evolved in the center of the spectrum, indicating the presence of frozen conformers.

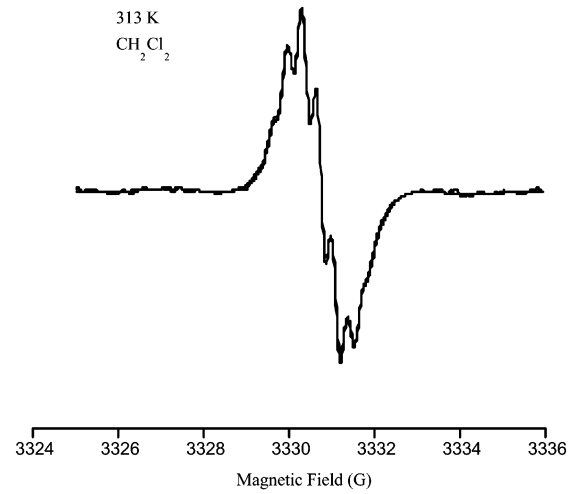

Figure 4. Experimental and calculated central line of the low-field nitrogen triplet for **c-1** showing the resolution of long-range couplings.

Below 133 K, anisotropic frozen solution spectra can be detected; further cooling to 103 K increased the line width. All of these spectral changes were reversible.

Significant solvent effects were also observed; better spectrum resolution was found in CH_2Cl_2 and benzene, where long-range proton couplings give a further multiplet structure. Simulations optimizing the square deviation between experimental and calculated spectra showed that eight hydrogens (six from the two methyl groups and two from the methylene groups) build up the multiplet structure (Figure 4).

Computer Simulations for Liquid Solution. For all ESR spectra of β-phosphorylated pyrrolidinoxyl radicals, the relative amplitudes of nitrogen triplet lines are different for the different quantum numbers of the phosphorus nuclei. This dependence can be described by two further relaxation parameters β' and γ', and the line widths were computed from the equation $\Delta H_{M,M'} = \alpha + \beta M + \gamma M^2 + \beta' M' + \gamma' MM'$, where M and M' represent the magnetic quantum numbers of nitrogen and phosphorus, respectively. The terms $\beta' M'$ and $\gamma' MM'$ are a consequence of the large anisotropy of the phosphorus hyperfine interaction. The ESR spectra were calculated with the automatic fitting procedure in which alternative algorithms were applied to achieve convergence in the least-squares process.[10] Between 333 and 143 K, the spectra of **c-1** were calculated by assuming a chemical exchange between two symmetric conformers. Ten parameters were adjusted, namely, the g factor, a_N, a_P^A, a_P^B, the exchange rate $k = 1/\tau$ as well as the five relaxation parameters α, β, γ, β', and γ'. At elevated temperature, the parameter fitting cannot give a reliable difference between a_P^A and a_P^B (Δa_P), which makes the determination of the exchange rate less precise. To obtain confident results in the high-temperature region, Δa_P was fixed at a value determined from spectra recorded below the coalescence temperature, and a nine-parameter fit was carried out. When they were resolved, long-range proton couplings and ^{13}C satellite lines were also simulated. The values of the adjusted hfsc and their temperature coefficients are listed in Table 1.

An Arrhenius plot of the exchange time showed good linearity (Figure 5), though above 303 K the exchange rate showed significant acceleration. The Arrhenius parameters in the low-temperature region are $E_a = 10.5$ kJ mol^{-1} and $k = 2.5 \times 10^{11}$ s^{-1} for $^1/_T = 0$.

Computer Simulations for Frozen Solution. Since the inclusion of rhombic parameters did not improve the quality of the fit significantly, the frozen solution spectra were simulated assuming axially symmetric **g**, $\mathbf{a}_N$, $\mathbf{a}_P^A$, and $\mathbf{a}_P^B$ tensors. For strain broadening, $\Delta H_{ii} = [\alpha_{ii} + \beta M + \gamma M^2]^{1/2}$, where $i = x, y$, or z,[10c] was taken in account by an axially symmetric α tensor, and β and γ were considered to be isotropic. Line shape was computed as a mixture of Lorentzian and Gaussian components. Altogether, 13 parameters were adjusted, and good agreement was observed between calculated and experimental spectra (Figure 6).

The average of the principal values of hyperfine tensors (Table 2) was rather close to the isotropic constants determined in liquid solution (Table 1).

The frozen-solution spectra showed significant ^{31}P anisotropy: for the axial phosphorus, the parallel component is larger than the perpendicular one by 8.8 G, whereas the opposite and a smaller difference (1.7 G) was observed for the equatorial phosphorus. The same trend was also observed by Chachaty et al.[11] for mono β-phosphorylated nitroxide radicals: when the isotropic ^{31}P hfsc was large ($a_P = 58-60$ G), the parallel component exceeded the perpendicular one by 7−8 G, whereas the difference was significantly smaller (4 G) when a_P was less than 40 G. This anisotropy cannot be explained by a direct

TABLE 1: Experimental and Calculated ESR Parameters for c-1 and t-1

c-1

	hfsc (G)		temp coeff (mG deg^{-1})		potential constants (kJ mol^{-1})	
	simulated	computed[c]	measured	computed[c]	V_1	V_2
a_N	14.06[a]		1.9[a]		8.5	15.0
a_P^A	46.97[a]	46.67	−11.2[a]	−10.5		
a_P^B	25.80[a]	25.63	−0.6[a]	0.2		
a_{Me}	0.36[b]					
$a_{H(CH2)}$	0.28[b]					

t-1

	hfsc (G)		temp coeff (mG deg^{-1})		potential constants (kJ mol^{-1})	
	simulated[d]	computed[c]	measured[d]	computed[c]	V_1	V_2
a_N	13.20				8.7	22.7
a_P	50.97	51.28	−11.2	−11.3		
a_{Me}	0.52					
$a_{H(CH2)}$	0.30					
$a_{H(CH2)}$	0.17[c]					

[a] In pentane. [b] In CH_2Cl_2. [c] Computed by the semiempirical approach. In CH_2Cl_2 $a_N = 14.5$ G, $a_P^A = 45.2$ G, $a_P^B = 27.16$ G, and ^{13}C couplings are 6.4 and 5.4 G. [d] In toluene.

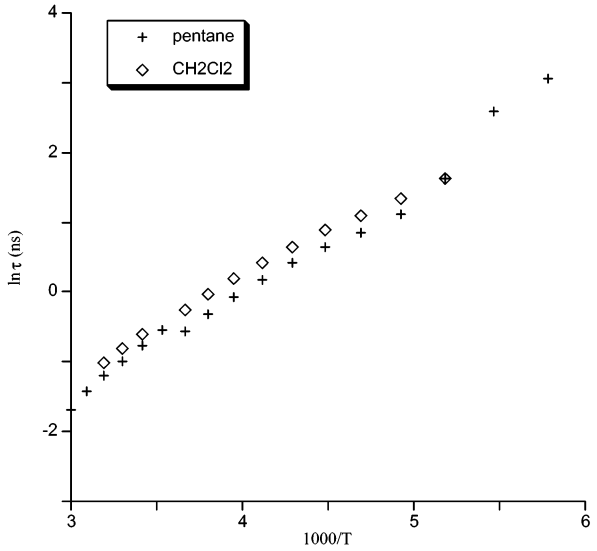

Figure 5. Arrhenius plot of the exchange time for **c-1**.

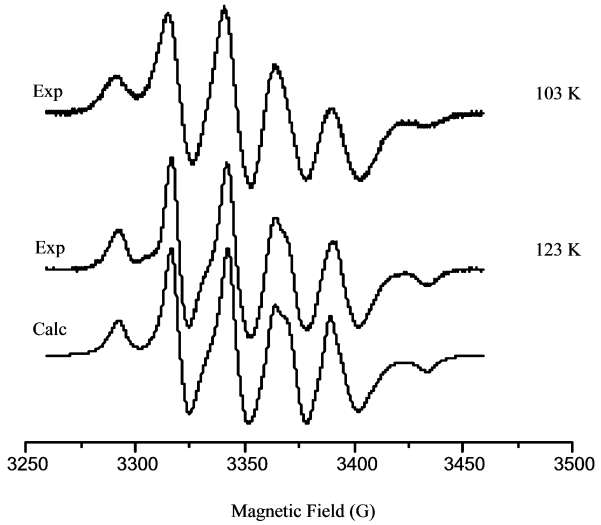

Figure 6. Experimental and calculated ESR spectra for **c-1** recorded in frozen *n*-pentane.

TABLE 2: g and hfsc Tensors for c-1 in Frozen *n*-Pentane

temp (K)	123	103
$\mathbf{g}_{\|}$	2.00221	2.00244
$\mathbf{g}_{\perp}$	2.00761	2.00757
$\mathbf{a}_{N_{\|}}$ (G)	30.8	29.6
$\mathbf{a}_{N\perp}$ (G)	5.0	7.0
$\mathbf{a}^{A}_{P\|}$ (G)	24.0	26.5
$\mathbf{a}^{A}_{P\perp}$ (G)	25.7	25.5
$\mathbf{a}^{B}_{P\|}$ (G)	55.1	56.0
$\mathbf{a}^{B}_{P\perp}$ (G)	46.3	42.3

dipolar interaction between the π unpaired electron and the ^{31}P nuclei. For a N−P distance of around 2.7×10^{-8} cm, the anisotropy should be smaller than 1 G. The large ^{31}P anisotropy could result from hyperconjugation between the singly occupied molecular orbital (SOMO) and the C−P bonds. Contrary to the case of the C−H bond, where spin density is transferred only to the 1s AO of hydrogen, the C−P bond spin density is transferred both to 3s and 3p AOs of phosphorus. As a consequence, the same Heller−McConnell[12]-type angular dependence should exist both for the isotropic and anisotropic hyperfine interactions; furthermore, the local symmetry axis for dipolar interaction should be parallel to the C−P bond. For the axial C−P bond, the dihedral angle is small, and the local symmetry axis is close to the principal direction of the unpaired electron density; therefore, $a_{||}$(P) is large. However, for the equatorial C−P bond, the local symmetry axis is almost perpendicular to the principal direction of the unpaired electron density, leading to larger $a_{\perp}$(P).

There is a significant difference between the frozen-solution spectra recorded at 133 and 103 K. At 133 K, the line shape is mainly Lorentzian (79% character), and at 103 K, it becomes mainly Gaussian (93% character). This trend can be explained by residual motion above 103 K.

Relaxation and Solvent Effects. The exchange rate also exhibited significant solvent dependence; it was somewhat larger in CH_2Cl_2. (The slope in the Arrhenius plot was the same, but its position was shifted.) This indicates complex formation between CH_2Cl_2 molecules and nitroxide radicals. The relaxation parameters for the nitrogen triplet ($\alpha + \beta M + \gamma M^2$) showed different behavior: although α was significantly larger in *n*-pentane, the β and γ parameters were slightly larger in CH_2Cl_2. The enhancement of α can be caused by a stronger spin−spin exchange in *n*-pentane that is due to the more frequent molecular encounters in a less viscous medium, whereas the increase in β and γ can be rationalized by a slower rotation in CH_2Cl_2 that is due to complex formation. The phosphorus relaxation given by β' and γ' was rather significant at low temperature, which indicates significant hyperfine anisotropy for β-phosphorus contrary to the case of β-hydrogen splitting. The presence of phosphorus relaxation was less clear for **c-1**, where chemical exchange is also present; however, for **t-1**, strongly different amplitude ratios were observed for the three nitrogen triplets. The sharpest lines were the central line and the first line in the low-field triplet and the high-field triplet, respectively.

Semiempirical Approach to the Pseudorotation of the Pyrrolidinoxyl Ring. We previously developed an ESR method utilizing the temperature dependence of β-^{13}C hfsc that gives quantitative information about the pseudorotation of pyrrolidinoxyl rings.[3] We assumed the following potential function

$$V = -\frac{1}{2}V_1[1 + \cos(\psi - \psi_1)] - \frac{1}{2}V_2[\cos(2(\psi - \psi_2))] \quad (1)$$

where ψ is the pseudorotation phase with a value set to zero for conformation $^3T_4$ (Figure 1). Because of the symmetry of **c-1**, $\psi_1 = \pi/2$, and $\psi_2 = 0$, and for a fixed puckering angle φ_0 (assumed to be ca. 40° from X-ray data[13]), all torsion angles and dihedral angles can be computed as a function of ψ.[14] We verified that the puckering angle affects the hfsc only slightly, thus its value is not critical within a wide range (between 30 and 45°).

The torsion angles are

$$\varphi_j = \varphi_0 \cos\left[\psi + \frac{4\pi}{5}(j-1)\right]$$

where the torsion angle is denoted by φ_j instead of the more conventional notation using four indices as $\varphi_{j-2,j-1,j+1,j+2}$. The dihedral angles of substituents on the C-2 and C-5 carbons are $\theta_2 = \pi/6 \pm \varphi_4$ and $\theta_5 = \pi/6 \pm \varphi_3$, respectively, where $\pm$ refers to the methyl or phosphoryl substituents.

The phosphorus coupling a_P was obtained from the simplified Heller−McConnell relation, $a_P = 58 \cos^2(\theta)$.[15] The mean value of $\cos^2(\theta)$ can be calculated by using the Boltzmann populations (eq 2) where the integration is carried out on the whole pseudorotational itinerary.

$$\langle\cos^2(\theta)\rangle = \frac{\int_0^{2\pi} \cos^2(\theta(\psi)) \exp\left(\frac{-V(\psi)}{kT}\right) d\psi}{\int_0^{2\pi} \exp\left(\frac{-V(\psi)}{kT}\right) d\psi} \quad (2)$$

In the presence of chemical exchange, the two interconverting sites can be represented by two potential wells separated by the potential barriers with pseudorotational phases ψ' and ψ''. Between these barriers, the rate of pseudo-oscillation around each minimum is still fast, whereas the chemical exchange is slowed by the hindrance of barriers. When $\langle\cos^2(\theta)\rangle$ is calculated from eq 2 for sites A and B, the integration limits are replaced

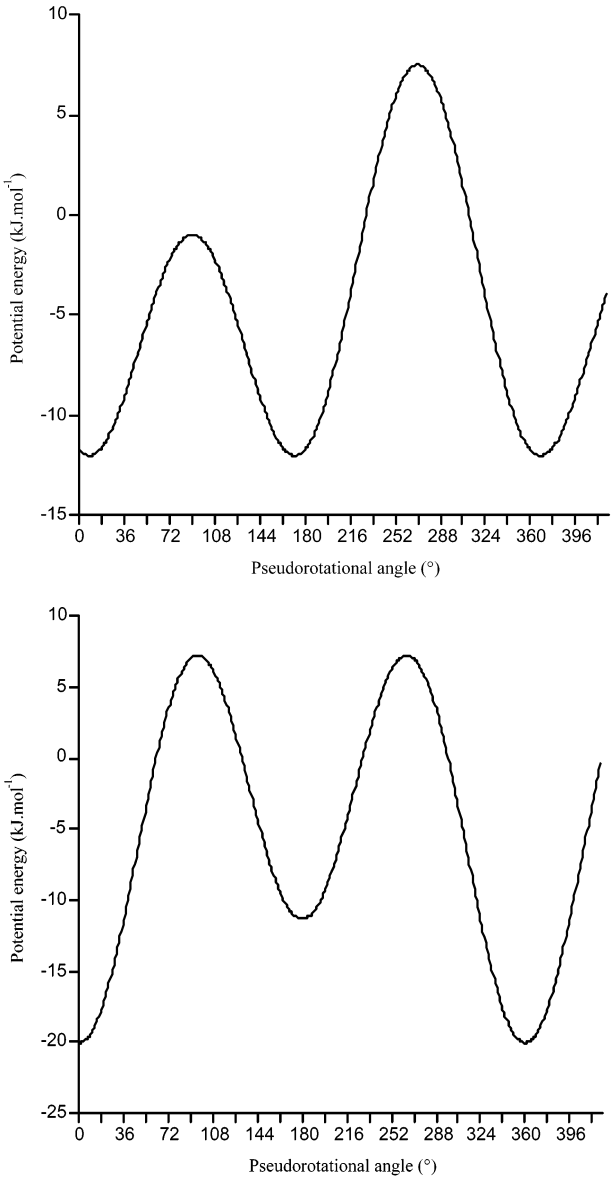

Figure 7. Empirical potential curve obtained according to eq 1 (left: **c-1**, right: **t-1**).

by [ψ', ψ''] and [ψ'', ψ'], respectively:

$$\langle\cos^2(\theta)\rangle_A = \frac{\int_{\psi'}^{\psi''} \cos^2(\theta(\psi)) \exp\left(\frac{-V(\psi)}{kT}\right) d\psi}{\int_{\psi'}^{\psi''} \exp\left(\frac{-V(\psi)}{kT}\right) d\psi} \quad (3a)$$

$$\langle\cos^2(\theta)\rangle_B = \frac{\int_{\psi''}^{\psi'} \cos^2(\theta(\psi)) \exp\left(\frac{-V(\psi)}{kT}\right) d\psi}{\int_{\psi''}^{\psi'} \exp\left(\frac{-V(\psi)}{kT}\right) d\psi} \quad (3b)$$

The rather large effective moment of inertia of the ring allows us to use a classical approach to describe the pseudorotation. Because of the symmetry of **c-1**, the potential minima should have identical energy, whereas the barriers can be different. On the contrary, for **t-1**, the barrier heights are identical, but the energy minima are different, allowing only a single populated conformer (Figure 7).

According to eq 1, the phosphorus hfsc depends on only two parameters, V_1 and V_2. Equations 1−3 allow us to determine both the hfsc and their temperature coefficients. Nonlinear least-squares iteration was used to find the V_1 and V_2 values giving the best agreement between experimental and calculated data (see Table 1). Altogether, four experimental data points—two hfsc and two temperature coefficients—were used to determine V_1 and V_2. The good agreement obtained for all data indicated the consistency of the applied model. Computations yielded potential amplitudes of $V_1 = 8.5$ kJ mol^{-1} and $V_2 = 15$ kJ mol^{-1}, whereas the positions of potential minima are $\psi_A = 8.3°$ and $\psi_B = 171.7°$, respectively. The phases of the minima indicate that the ground conformers have intermediate geometry between $^3T_4$ and ^3E or $^4T_3$ and ^4E. Note that the molecular symmetry defines only the positions of the potential maxima, but the positions of the minima are not defined! The potential barriers separating potential wells are found to be 11.0 and 19.6 kJ mol^{-1}. The smaller value is remarkably close to the barrier of 10.5 kJ mol^{-1} that was obtained from the Arrhenius plot (Figure 5) of the exchange rate in the low-temperature region, and it also agrees with the potential barrier determined by the analysis of ^{13}C hfsc for the 2,2,5,5-tetramethyl-pyrrolidine-1-oxyl radical.[3]

The Arrhenius curve showed an increased slope at high temperature. This increase can be explained by an alternative route of ring inversion: a puckering vibration through the planar structure. According to microwave spectroscopy,[5] the barrier of this inversion process is rather high, but because of the large entropy of this motion, it can be faster than the pseudorotation at elevated temperature. (Note that in the course of inversion pseudorotational motion requires a series of well-defined molecular geometries, whereas any two puckered conformations could be directly interconverted via the planar ring geometry.)

As a comparison, the same analysis was carried out for **t-1**. In this case, the two energy minima have exact $^3T_4$ and $^4T_3$ geometries, but the former has significantly larger energy (8.7 kJ mol^{-1}, see Table 1). For this reason, only one conformer is populated, and no chemical exchange can occur.

Conformational Analysis by Molecular Mechanics. The results obtained from the above semiempirical approach have been compared with the results derived from molecular mechanics calculations. For this purpose, we used GenMol software[16] that includes the parameters for an aminoxyl moiety.[4,17] Moreover, the method developed by Cremer and Pople[18] has been implemented in GenMol for a quantitative conformational analysis of five-membered rings.[4] This method is based on the definition of a mean plane, which is invariant during the pseudorotation. For any conformation of the ring, the z_j coordinate of the jth atom of the ring measures its distance to the mean plane and is written

$$z_j = \sqrt{\frac{2}{5}} q \sin\left(\frac{4\pi(j-1)}{5} + \psi\right) \qquad \psi \in [0; 2\pi]$$

$q \in [0.3; 0.5](10^{-8}$ cm)

for most of the five-membered rings

With any values of the puckering amplitude q and pseudorotation angle ψ, the corresponding conformation of a five-membered ring can be automatically built by GenMol. The same kind of strategy was used by French and Tran[19] to analyze the fructofuranose conformations with the MMP2(85) program.

For **t-1** and **c-1**, the 20 ideal-ring conformers (10 envelopes and 10 twists) equally spaced by 18° on the pseudorotation circle were generated (Figure 1). Around each C−P bond, three staggered rotamers a, g−, and g+ were considered (Scheme 2). Therefore, for each envelope or twist conformer, 9 ideal

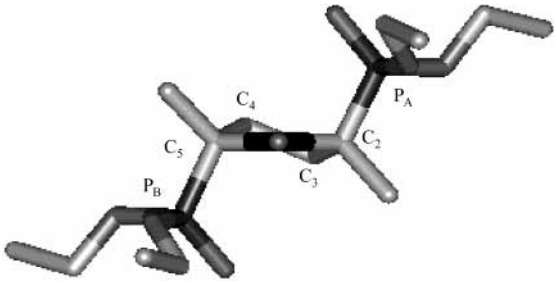

Figure 8. Preferred geometry of **t-1** obtained from molecular mechanics.

SCHEME 2: g+, g−, and a Orientations of the Diethoxyphosphoryl Groups

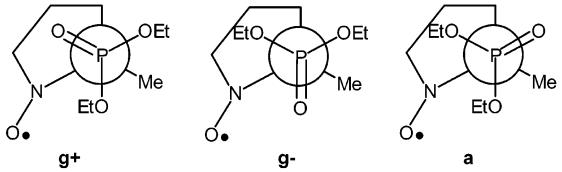

TABLE 3: Results of the Preliminary Conformational Analysis of t-1

	$E_{steric}(^4T_3)$ (kJ mol^{-1})	population (273 K) (%)	q (10^{-8} cm)	ψ (deg)	a_P^A (G)	a_P^B (G)
g−g−	**84**	**42.8**	**0.37**	**177**	**53.6**	**52.2**
aa	90	3.0	0.36	178	52.8	52.2
g+g+	93	0.8	0.36	177	52.3	51.2
ag−	86	17.7	0.35	174	54.6	50.8
g−a	86	17.7	0.36	184	50.8	54.4
g−g+	88	7.3	0.37	180	52.0	52.9
g+g−	88	7.3	0.36	182	52.2	52.7
ag+	91	2.0	0.36	178	52.3	51.9
g+a	92	1.3	0.35	177	52.7	51.4
mean values			0.36	178	52.9	52.4

rotamers (aa, ag+, ag−, g+a, g−a, g+g+, g+g−, g−g+, g−g−) must be considered, and for either **t-1** or **c-1**, 180 conformations were generated. These conformations were then optimized in the GenMol force field up to the convergence limit of 0.005 kJ mol^{-1} using the following procedure.

Each conformation was built with an arbitrary puckering amplitude (0.4 10^{-8} cm), and the geometry of the ethoxyl chains was first optimized by a local conformational analysis (the remaining atoms being fixed). Then, the geometry optimization of the whole molecule was performed. For **t-1** and **c-1**, the energy minima that were found correspond to $^3T_4$ and $^4T_3$ conformers, and the energy maxima, to ^1E and E_1 conformers.

Conformational Analysis for t-1. The analysis showed that the orientation of the diethoxyphosphoryl substituents can only slightly change the geometry of ground $^3T_4$ and $^4T_3$ conformers. For each kind of rotamer, the $^4T_3$ conformer with pseudoaxial phosphorus atoms was largely favored. We obtained a value of $\langle\psi\rangle = 178°$, which is close to the value calculated by the semiempirical approach ($\langle\psi\rangle = 180°$). The energy difference between the $^4T_3$ and $^3T_4$ conformers was found to be around 10 kJ mol^{-1}, in good agreement with the value obtained by the analysis of ^{31}P hfsc (8.7 kJ mol^{-1}, see Table 1). The results of the calculations for the $^4T_3$ rotamers are shown in Table 3. For the most favored rotamer (g−g−), the ethoxyl fragments are as far as possible from the ring to reduce steric interactions (Figure 8).

TABLE 4: Results of the Conformational Analysis of c-1[a]

	minimum 1 ($^4T_3$ or E_3)			minimum 2 ($^3T_4$ or E_4)		
	E_{steric} (kJ mol^{-1})	q (10^{-8} cm)	ψ (deg)	E_{steric} (kJ.mol^{-1})	q (10^{-8} cm)	ψ (deg)
aa	89	0.37	173	89	0.37	6
g+g−	91	0.36	173	91	0.36	8
g−g+	92	0.36	181	92	0.36	−2
g+g+	*94*	*0.35*	*165*	*90*	*0.36*	*2*
g−g−	90	0.36	179	94	0.36	14
ag−	88	0.36	174	92	0.35	−1
g+a	92	0.35	180	88	0.36	6
ag+	96	0.37	175	88	0.36	6
g−a	88	0.36	173	96	0.37	5
mean values			174.5			5.2

[a] Envelopes are in italics.

Conformational Analysis for c-1. As already mentioned, the conformational study gave two potential wells around the $^3T_4$ and $^4T_3$ conformations. However, for the nine rotamers, the phase minima were shifted, suggesting an intermediate geometry between $^4T_3$ and E_3 ($\langle\psi\rangle = 174.5°$) or $^3T_4$ and E_4 ($\langle\psi\rangle = 5.2°$), respectively (Table 4). Molecular mechanics calculations are then in agreement with the results of the above semiempirical model ($\psi = 171.8$ and 8.3° respectively). The type of rotamer can influence the energy minima up to 8 kJ mol^{-1}. According to C_v symmetry, the aa, g+g− and g−g+ rotamers of the $^3T_4$ and $^4T_3$ conformers are mirror images (Figure 9), whereas for the rotamer pairs (g+g+, g−g−), (ag−, g+a) and (ag+, g−a) the symmetry exists if one of the rotamers is combined with $^3T_4$ and the other, with $^4T_3$ (ag−/$^4T_3$ ↔ g+a/$^3T_4$).

The interconversion between the symmetric $^3T_4$ and $^4T_3$ conformers can take place either through inversion via a planar ring or by the pseudorotational process. In both cases, the molecular geometry should change through intricate geared motions including ring distortion, rotation around the C−P bonds, and reorientation of the ethoxyl chains.

To calculate the potential barrier, the nine E_1 rotamers and the nine ^1E rotamers were built with an initial puckering

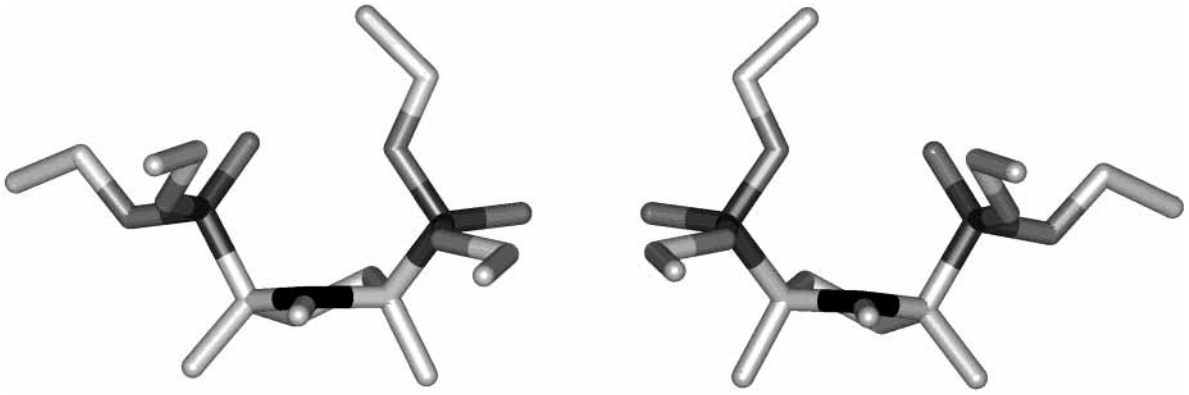

Figure 9. ag−/$^4T_3$ and g+a/$^3T_4$ symmetric conformers of **c-1**.

amplitude of 0.3×10^{-8} cm. Starting from these 18 initial rotamers, the puckering amplitude was then systematically varied between 0 and 0.7×10^{-8} cm, and the most stable E_1 and ^1E conformations were determined. Mainly because of steric repulsion between the axially oriented phosphoryl groups, we found that the ^1E conformers had larger energy. Computations suggested that for the most stable E_1 geometry the ring was almost planar ($q = 0.11 \times 10^{-8}$ cm) and the energy was 25 kJ mol^{-1} higher than the energy of the most favored $^3T_4$ or $^4T_3$ conformer. Hence, molecular mechanics yields for the exchange process a significantly larger barrier than that derived from the temperature dependence of either the interconversion rate (10.5 kJ mol^{-1}) or the phosphorus hfsc (11.1 kJ mol^{-1}).

Conclusions

The temperature dependence of the ESR spectrum for *cis*- and *trans*-2,5-diphosphoryl-2,5-dimethyl-pyrrolidinoxyl radicals **c-1** and **t-1**, respectively, was studied over a large temperature range. For **t-1**, line-width changes can be explained by the expected relaxation processes. However, for **c-1**, dramatic changes in the hyperfine pattern were observed and attributed to an interconversion between two symmetric conformations separated by a potential barrier. The large difference in the two phosphorus hfsc ($\Delta A_P \approx 21$ G) accounts for the unusually large alternating line broadening observed at high temperature. In the low-temperature region, the temperature dependence of the interconversion rate gives a potential barrier of 10.5 kJ mol^{-1}. At elevated temperature, an acceleration of the exchange rate shows that interconversion could also take place by alternative routes. Although at low temperature the major process is a pseudorotation with a small energy barrier and a small entropy value, at high temperature, a puckering vibration through the planar structure could be predominant, where both the barrier and the entropy are larger. The significant decrease of the exchange rate observed in methylene chloride could result from complexation.

Apart from the "dynamic" phenomenon of chemical exchange, the population averaging of conformers in the pseudorotational itinerary was also studied via the phosphorus couplings and their temperature coefficients. This analysis yielded a 11.1 kJ mol^{-1} potential barrier for pseudorotation, which was in a remarkably good agreement with the value derived from the dynamic model. Computation suggests that the pseudorotation has two minima with geometry that corresponds to an "intermediate" structure between conformers $^3T_4$ and ^3E as well as between conformers $^4T_3$ and E_3.

Molecular mechanics computations were in a good agreement with the semiempirical potential derived from ESR data. Both for **t-1** and **c-1** the major characteristics of the potential function are well reproduced, even though the value of the potential barrier is overestimated by a factor of 2. Rotation around the C−P bonds can significantly affect the size of the potential barrier but cannot modify the geometries of ground ring conformations.

In the frozen-solution spectra of **c-1**, fairly large hfsc anisotropy was observed for the pseudoaxial phosphorus atom, whereas for the pseudoequatorial phosphorus the anisotropy was smaller. Hyperconjugation between the SOMO and the C−P bonds can explain not only the large isotropic hfsc but also the conformational dependence of the phosphorus anisotropy.

Experimental Section

ESR measurements were performed on a Bruker ESP 300 spectrometer equipped with a TM 110 cavity and an X-band resonator (9.41 GHz). All ESR spectra were recorded at 100-kHz magnetic field modulations. The ESR samples (10^{-5} M in nitroxide) were deoxygenated by freeze and thaw cycles.

Cis- and *trans*-2,5-diethoxyphosphoryl-2,5-dimethylpyrrolidinoxyl radicals were isolated after the oxidation of the corresponding pyrrolidines.[20] *n*-Pentane (99%), methylene chloride (99.9%), and toluene (99.5%) were from SDS (France) and were used as received.

Acknowledgment. We thank the Hungarian Scientific Research Fund OTKA (grant T-032929), the CNRS, and the French Ministry of Research for financial support.

References and Notes

(1) (a) McCarren, P. R.; Gordon, M. T.; Lowary, T. L.; Hadad, C. M. *J. Phys. Chem. A* **2001**, *105*, 5911. (b) Gordon, M. T.; Lowary, T. L.; Hadad, C. M. *J. Org. Chem.* **2000**, *65*, 4954. (c) Gordon, M. T.; Lowary, T. L.; Hadad, C. M. *J. Am. Chem. Soc.* **1999**, *121*, 9682. (d) Ma, B.; Schaefer, H. F., III; Allinger, N. L. *J. Am. Chem. Soc.* **1998**, *120*, 3411. (e) Bandyopadhyay, T.; Wu, J.; Stripe, W. A.; Carmichael, I., Serianni, A. S. *J. Am. Chem. Soc.* **1997**, *119*, 1737. (f) Cros, S.; Hervé du Penhoat, C.; Pérez, S.; Imberty, A. *Carbohydr. Res.* **1993**, *248*, 81. (g) Cros, S.; Imberty, A.; Bouchemal, N.; Hervé du Penhoat, C.; Pérez, S. *Biopolymers* **1994**, *34*, 1433.

(2) (a) Dzakula, Z.; DeRider, M. L.; Markley, J. L. *J. Am. Chem. Soc.* **1996**, *118*, 12796. (b) Haasnoot, C. A. G.; de Leeuw, F. A. A. M.; de Leeuw, H. P. M.; Altona, C. *Biopolymers* **1981**, *20*, 1211. (c) de Leeuw, F. A. A. M.; Altona, C.; Kessler, H.; Bermel, W.; Friedrich, A.; Krack, G.; Hull, W. E. *J. Am. Chem. Soc.* **1983**, *105*, 2237.

(3) Rockenbauer, A.; Korecz, L.; Hideg, K. *J. Chem. Soc., Perkin Trans. 2* **1993**, 2149.

(4) Siri, D.; Gaudel-Siri, A.; Tordo, P. *J. Mol. Struct.: THEOCHEM* **2002**, *582*, 171.

(5) (a) Malloy, T. B., Jr.; Bauman, L. E.; Carreira, L. A. *Top. Stereochem.* **1979**, *11*, 97−185. (b) Kim, H.; Gwinn W. *J. Chem. Phys.* **1969**, *51*, 1815.

(6) (a) Roberts, B. P.; Steel, A. J. *J. Chem. Soc., Perkin Trans. 2* **1992**, 2025. (b) Rolfe, R. E.; Sales, K. D.; Utley, J. H. P. *J. Chem. Soc., Perkin Trans. 2* **1973**, 1171. (c) Windle, J. J.; Kuhnle, J. A.; Beck, B. H. *J. Chem. Phys.* **1969**, *50*, 2630. (d) Ogawa, S.; Fessenden, R. W. *J. Chem. Phys.* **1964**, *41*, 994.

(7) Shiotani, M.; Sjöqvist, L.; Lund, A.; Lunell, S.; Eriksson, L.; Huang, M. B. *J. Phys. Chem.* **1990**, *94*, 8081.

(8) (a) Sjöqvist, L.; Lund, A.; Maruani, J. *Chem. Phys.* **1988**, *125*, 293. (b) Sjöqvist, L.; Lindgren, M.; Lund., A. *Chem. Phys. Lett.* **1989**, *156*, 323. (c) Kubuzono, Y.; Okada, M.; Aoyagi, M.; Yahiro, S.; Nakamura, H.; Matsuo, T. *Z. Naturforsch., A: Phys. Sci.* **1991**, *46*, 993.

(9) (a) Fréjaville, C.; Karoui, H.; Tuccio, B.; Le Moigne, F.; Culcasi, M.; Pietri, S.; Lauricella, R.; Tordo, P. *J. Chem. Soc., Chem. Commun.* **1994**, 1793. (b) Fréjaville, C.; Karoui, H.; Tuccio, B.; Le Moigne, F.; Culcasi, M.; Pietri, S.; Lauricella, R.; Tordo, P. *J. Med. Chem.* **1995**, *38*, 258. (c) Rockenbauer, A.; Mercier, A.; Le Moigne, F.; Olive, G.; Tordo, P. *J. Phys. Chem.* **1997**, *101*, 7965.

(10) (a) Rockenbauer, A.; Korecz, L. *Appl. Magn. Reson.* **1996**, *10*, 29. (b) Rockenbauer, A. *Mol. Phys. Rep.* **1999**, *26*, 117. (c) Rockenbauer, A.; Simon, P. *J. Magn. Reson.* **1975**, *18*, 320.

(11) Chachaty, C.; Mathieu, C.; Mercier, A.; Tordo, P. *Magn. Reson. Chem.* **1998**, *36*, 46.

(12) Heller, C.; McConnell, H. M. *J. Chem. Phys.* **1960**, *32*, 1535.

(13) (a) Ament, S. S.; Wetherington, J. B.; Moncrief, J. W.; Flohr, K.; Mochizuki, M.; Kaizer, E. T.; *J. Am. Chem. Soc.* **1973**, *95*, 7896. (b) Wetherington, J. B.; Ament, S. S.; Moncrief, J. W. Acta *Crystallogr., Sect. B* **1974**, *30*, 568. (c) Chion, B.; Lajzerowicz, J. *Acta Crystallogr., Sect. B* **1975**, *31*, 1430. (d) Chion, B. *Cryst. Struct. Commun.* **1978**, *7*, 395. (e) Chion, B.; Lajzerowicz, J.; Collet, A.; Jacques, J. *Acta Crystallogr., Sect. B* **1976**, *32*, 339. (f) Keana, J. F.; Hideg, K.; Birrel, G. B.; Hankovszky, O. H.; Ferguson, G.; Parvez, M. *Can. J. Chem.* **1982**, *60*, 1439.

(14) Altona, C.; Sundaralingam, M. *J. Am. Chem. Soc.* **1972**, *94*, 8205.

(15) Dembrowski, L.; Finet, J.-P.; Fréjaville, C.; Le Moigne, F.; Maurin, R.; Mercier, A.; Pages, P.; Stipa, P.; Tordo, P. *Free Radical Res. Commun.* **1993**, *19*, S23.

(16) Pèpe, G.; Siri, D. *Stud. Phys. Theor. Chem.* **1990**, *11*, 411.

(17) Vila, F.; Tordo, P.; Siri, D.; Pèpe, G. *Free Radical Res. Commun.* **1993**, *19*, S17.

(18) (a) Cremer, D.; Pople, J. A. *J. Am. Chem. Soc.* **1975**, *97*, 1354. (b) Essen, H.; Cremer, D. *Acta Crystallogr., Sect. B* **1984**, *40*, 418. (c) Cremer, D. *J. Phys. Chem.* **1990**, *94*, 5502.

(19) French, A. D.; Tran, V. *Biopolymers* **1990**, *29*, 1599.

(20) Le Moigne, F.; Tordo, P. *C. R. Acad. Sci.* **2001**, *4*, 585−590.